

# Human intraretinal myelination: Axon diameters and axon/myelin thickness ratios

Thomas FitzGibbon<sup>1,2</sup>, Zoran Nestorovski<sup>1,3</sup>

**Purpose:** Human intraretinal myelination of ganglion cell axons occurs in about 1% of the population. We examined myelin thickness and axon diameter in human retinal specimens containing myelinated retinal ganglion cell axons. **Materials and Methods:** Two eyes containing myelinated patches were prepared for electron microscopy. Two areas were examined in one retina and five in the second retina. Measurements were compared to normal retinal and optic nerve samples and the rabbit retina, which normally contains myelinated axons. Measurements were made using a graphics tablet. **Results:** Mean axon diameter of myelinated axons at all locations were significantly larger than unmyelinated axons ( $P \leq 0.01$ ). Myelinated axons within the patches were significantly larger than axons within the optic nerve ( $P < 0.01$ ). The relationship between axon diameter/fiber diameter (the G-ratio) seen in the retinal sites differed from that in the nerve. G-ratios were higher and myelin thickness was positively correlated to axon diameter ( $P < 0.01$ ) in the retina but negatively correlated to axon diameter in the nerve ( $P < 0.001$ ). **Conclusion:** Intraretinally myelinated axons are larger than non-myelinated axons from the same population and suggests that glial cells can induce diameter changes in retinal axons that are not normally myelinated. This effect is more dramatic on intraretinal axons compared with the normal transition zone as axons enter the optic nerve and these changes are abnormal. Whether intraretinal myelin alters axonal conduction velocity or blocks axonal conduction remains to be clarified and these issues may have different clinical outcomes.

**Key words:** Axon diameter, electron microscopy, nerve fiber layer, oligodendrocytes, pathology

In general, mammalian retinal ganglion cell axons are not myelinated and evidence suggests that factors at the lamina cribrosa may block the migration of oligodendrocyte precursors beyond the retinal-optic nerve junction (ROJ).<sup>[1-4]</sup> However, intraretinal myelination (IRM) occurs in ~0.5 to 1% of humans<sup>[5-7]</sup> and does occur in normal animals with a lamina cribrosa.<sup>[2,8]</sup> IRM appears as white or opaque areas in the nerve fiber layer, tends to be unilateral showing no preference for either eye, affects males and females equally<sup>[5,9-11]</sup> and has a number of ocular and associated visual problems (e.g. amblyopia).<sup>[6,7,9-11]</sup> IRM is thought to be more common in the elderly, but the origin and time course remain unknown.

Myelin sheath thickness and internodal length in mature nerves are proportional to axon diameter and there is a positive correlation between myelin thickness and neurofilament dynamics.<sup>[12,13]</sup> Axon diameter may be a significant factor in the myelination process and larger optic nerve (ON) axons are myelinated first.<sup>[12,14-16]</sup> It is unclear whether interactions between axons and oligodendrocytes are regulated by cell-cell contact, diffusible factors, or a combination of interactions.<sup>[4,17-19]</sup>

IRM provides a rare opportunity to examine whether the relationship between axon size and myelin thickness is affected by the site of myelination. We used electron microscopy to

analyze axon diameter and myelin thickness in IRM and ON. We also compared these values to normal IRM in the rabbit, which lacks a lamina cribrosa and has naturally occurring IRM along the visual streak.<sup>[16,20]</sup> While the present study largely focuses on basic research we provide some likely clinical outcomes resulting from the intraretinal myelination.

## Materials and Methods

Human tissue was obtained postmortem from the Lions Eye Bank in Sydney. All experiments were done in accordance with ethical approval from Human Ethics Committee in Sydney. Examination of a large number of donor eyes (the department has several hundred eyes in their collection) revealed two eyes with myelinated patches; the companion eyes appeared normal. The donors were female aged 80 and 85-years old (S656 and S694) and the delays to fixation were 24 and 12 h, respectively. A nonmyelinated retina from a 77 year old female (fixation delay 20 h) was used for comparison. The corneas were removed for transplants, and then the eyecups stored in 2-4% paraformaldehyde in 0.1M phosphate buffer (pH 7.4) at 4°C. Ophthalmic histories were not available. Previous work demonstrated that adequate tissue and ultrastructural preservation could be achieved with this protocol.<sup>[21,22]</sup>

Retinal tissue blocks of ~1-2 mm<sup>2</sup> were removed from different locations using a scalpel blade. Care was taken to ensure that peripheral and central samples were taken at points within the retina that contained the same axonal population. Blocks were processed for routine electron microscopy as described elsewhere.<sup>[21,23]</sup> Sections were examined using a Hitachi H500 electron microscope. Micrographs were printed at a final magnification between 3,000 and 14,000 times. Axonal area was measured using a graphics tablet and an in-house designed computer morphometrics package;<sup>[24]</sup> the area was

Access this article online

Website:

www.ijo.in

DOI:

10.4103/0301-4738.121075

Quick Response Code:



<sup>1</sup>Department of Clinical Ophthalmology, and <sup>2</sup>School of Medical Sciences and Bosch Institute, Discipline of Anatomy and Histology, and <sup>3</sup>School of Orthoptics, University of Sydney, NSW 2006 Australia

**Correspondence to:** Dr. Thomas FitzGibbon, Department of Biomedical Engineering, A-502, Peking University Hospital, Peking University, Beijing 100 871, China. E-mail: tomf@physiol.usyd.edu.au

Manuscript received: 07.02.12; Revision accepted: 20.05.13

then converted to the diameter of a circle with an equivalent area. Axon diameter was defined as the *axon diameter excluding myelin* [ad in Fig. 1], in contrast to fiber diameter which was defined as *axon diameter plus myelin* [fd in Fig. 1]. In cases of disrupted myelin, the thickness was measured from compact regions of the myelin [e.g. Fig. 2F]. The g-ratio was defined as the axon diameter (ad) divided by the fiber diameter (fd) and provides a structural and functional index of what might be considered as optimal axonal myelination. Samples were considered significantly different with  $P \leq 0.05$  (two way *t*-test or correlation coefficient).

Adult rabbit retinas were obtained after unrelated experiments and had prior ethical approval from Human Ethics Committee in Sydney. Rabbits were given a lethal dose of sodium pentobarbital and perfused through the heart with saline followed by 4% paraformaldehyde in 0.1M phosphate buffer. The eyecups were stored in the same fixative, and then processed as above for human material.

## Results

Areas containing IRM patches in the human retina were easily seen with an ophthalmoscope or dissecting microscope as whitish or opaque areas within the nerve fiber layer (subsequent electronmicroscopy confirmed the presence of myelinated axons). These patches did not have sharply delineated peripheral or central borders, were variable in size and shape (up to ~ 3 mm in length), and generally found along the arcuate bundles.<sup>[5-7,11]</sup> There were less myelinated fibers within transition zones (i.e. edges of the patch)<sup>[23]</sup> compared to regions closer to the disc (similar to the rabbit retina).<sup>[16,20]</sup> In contrast to the rabbit, human IRM was not continuous with ON myelination. The lamina cribrosa contained very few myelinated fibers and did not appear to differ from normal material.<sup>[5-7,11]</sup> Myelinated fibers were not strictly confined to specific retinal fascicles or locations within a fascicle, nor were they always associated with blood vessels. Thus, there did not appear to be any constraints on the location or limits to the myelination.<sup>[23]</sup>

IRM patches contained a mixture of myelinated and unmyelinated axons with a range of morphological features from normal to late stages of degeneration [Fig. 2]. It is not

certain, but we believe this degeneration was specific to the IRM and was not related to age. There was very little evidence for the presence of an inflammatory reaction within the nerve fiber layer.<sup>[23]</sup> However, in all cases, normal well-preserved axons were interspersed between these degenerating profiles.<sup>[12,20,25,26]</sup> Fibers that showed signs of myelin rejection were not always associated with obvious degenerative changes in the axons.

Comparison between subjects revealed that mean unmyelinated axon diameters in S656 were significantly larger than those of S694 ( $0.62 \pm 0.50$   $n = 1149$  vs.  $0.70 \pm 0.46$   $n = 1565$ , respectively;  $P < 0.01$ ) [Figs. 3 and 4]. Because of this and the fact that axon diameter varies with retina location,<sup>[27]</sup> comparisons within each eye will be dealt with separately. Mean unmyelinated axon diameter in S694 [Fig. 3] significantly increased between the peripheral (R1,  $0.50 \pm 0.35$   $\mu\text{m}$ ) and more heavily myelinated central sample (R2,  $0.95 \pm 0.57$   $\mu\text{m}$ ;  $P \leq 0.01$ ). Myelinated axon size also significantly increased between peripheral and central samples (R1,  $0.62 \pm 0.30$  vs. R2,  $1.59 \pm 0.81$   $\mu\text{m}$ ,  $P \leq 0.01$ ), but were only significantly larger than unmyelinated axons in the central sample ( $P \leq 0.01$ ). The range of fiber sizes seen in the central sample (R2) was also greater than that seen in the peripheral sample (R1).

In S694, blocks were prepared from the peripheral retina (R1 ~ 10 mm temporal from the optic disc (OD) Fig. 4), in the IRM patch (R2 ~ 2 mm from the OD), the lamina cribrosa (R3), the ROJ (R4; a region of normal transition from unmyelinated to myelinated axons), and the ON (R5; Figs. 4 and 5). In order to sample the same population of axons at each location, the embedded tissue block included the retina, ROJ and ON. Sections were obtained for each location by serially cutting thick and thin section from the block; the block was periodically reoriented to maintain a cutting surface at right angles to the long axis of the axons. Mean unmyelinated axon diameters increased from the peripheral sample (R1,  $0.69 \pm 0.59$   $\mu\text{m}$ ) to the lamina cribrosa (R3,  $0.89 \pm 0.71$   $\mu\text{m}$ ;  $P \leq 0.01$ ) but peripheral axons were not significantly different from axons in the ROJ (R4,  $0.66 \pm 0.41$   $\mu\text{m}$ ). The significantly larger axon diameters in the lamina cribrosa (R3) suggest that the axons have not completely returned to their original diameter and are still influenced by the presence of IRM. In contrast, myelinated axons were larger in IRM patch (R2,  $1.37 \pm 1.22$   $\mu\text{m}$ ) compared with the

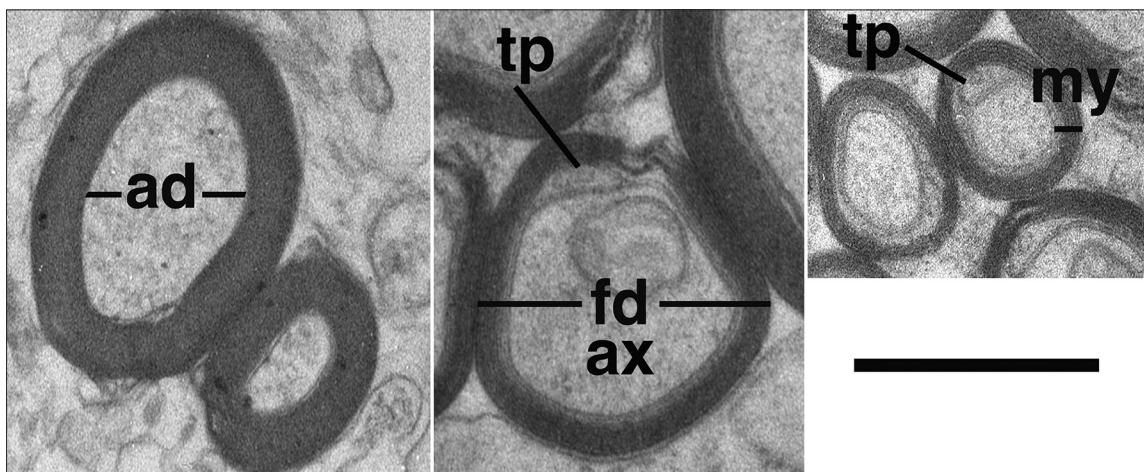


**Figure 1:** Examples are shown of the measurements used for analysis of g-ratio ( $ad/fd =$  axon diameter/fiber diameter) and myelin thickness (my). The internal tongue process (tp) of the myelin wrapping is indicated surrounding the axon (ax). Bar 0.5  $\mu\text{m}$



ROJ (R4,  $0.96 \pm 0.55 \mu\text{m}$ ) and ON (R5,  $0.74 \pm 0.38 \mu\text{m}$ ;  $P \leq 0.01$ ); mean axon diameter of myelinated axons at all locations were significantly larger than unmyelinated axons ( $P \leq 0.01$ ).

It seems clear that unmyelinated axons in the IRM patches have larger diameters (and a broader range) and this may depend on the density of neighboring myelinated axons. In addition, axon diameter increases once the axon becomes myelinated. However, the difference between unmyelinated and myelinated axon diameters seemed to be greater in regions of dense IRM (~45% increase) compared to the normal transition zone from un- to myelinated axons (the ROJ, ~30% increase). Myelination at the ROJ does not occur at the same level for all axons but the number of myelinated axons gradually increases with distance along the ON. Although the ROJ and IRM patches were similar in this respect, there were marked differences in mean myelinated axon sizes. Mean axon diameter of myelinated IRM fibers was significantly larger ( $P \leq 0.05$ ) and the range broader compared to the ROJ (range 0.1-8.5 vs. 0.2-2.4  $\mu\text{m}$ , respectively). In contrast, unmyelinated axons in these two regions were not significantly different. In S656 there was a significant increase in ON axon diameter ( $P \leq 0.01$ ) compared to unmyelinated retinal areas (an ~10% increase between the retina/ROJ and ON). Mean ON axon diameters were similar to previous reports if myelin thickness is included (S656:  $0.99 \pm 0.38 \mu\text{m}$ ).<sup>[25]</sup> Clearly the intraretinal fiber diameters (S694:  $1.95 \pm 0.83 \mu\text{m}$ ; S656:  $1.63 \pm 1.24 \mu\text{m}$ ) were larger than those seen in the ON of the present study and reported by others, although the presence of particularly large retinal axons in humans<sup>[28]</sup> and other species<sup>[16,29,30]</sup> has been reported.

Mean myelin thickness in S694 [Fig. 3] was significantly thinner in the more lightly myelinated region compared with the more heavily myelinated patch closer to the optic disc (R1,  $0.09 \pm 0.03 \mu\text{m}$  vs. R2,  $0.18 \pm 0.05 \mu\text{m}$ ,  $P \leq 0.01$ ). Myelin thickness and axon diameter were not correlated within the

patches ( $P = 0.34$ ). The g-ratios (axon diameter (ad)/fiber diameter (fd); see Fig. 1) were not significantly different for the two sampled regions ( $0.78 \pm 0.12 \mu\text{m}$ , combined sample).

Mean myelin thickness in the IRM patch of S656 ( $0.13 \pm 0.03 \mu\text{m}$ ; Fig. 4) was not significantly different from ON measurements ( $0.12 \pm 0.05 \mu\text{m}$ ); however, ROJ myelin ( $0.07 \pm 0.03 \mu\text{m}$ ) was significantly thinner when compared to both these locations ( $P \leq 0.05$ ), that is, areas representing a transition between unmyelinated and myelinated fibers (S694R1 and ROJ of S656R4). The myelin thickness in S656 was on average thinner than that measured in the normal ON ( $0.19 \pm 0.05 \mu\text{m}$ ,  $n = 745$ ) and the more densely myelinated patch of S694 (R2, 0.18).

The increase in myelin thickness was positively correlated to axon diameter in the IRM patch (S656: R2,  $r^2 = 0.03$ ,  $P < 0.001$ ) and the ROJ (R4;  $r^2 = 0.07$ ,  $P = 0.01$ ). In contrast, within the ON of S656 (R5) and the normal sample these variables were negatively correlated ( $r^2 = 0.01$ ,  $P < 0.001$ ;  $r^2 = 0.008$ ,  $P = 0.02$ , respectively), that is, myelin thickness decreases as axon diameter increases. The g-ratios in the IRM ( $0.79 \pm 0.12$ ) were very similar to those seen in S694 and within the ON ( $0.73 \pm 0.12$ ). As expected, due to the thinner ROJ myelin, the g-ratios ( $0.84 \pm 0.09$ ) were higher than seen elsewhere. The mean ON g-ratio (S656) was significantly higher than in the normal ON ( $0.58 \pm 0.14$ ) and this may be attributed to a higher proportion of larger ON axons of S656. Scatter plots of individual g-ratios in the normal subject plateau at ~0.85 once the axonal diameter reaches 1-1.5  $\mu\text{m}$ ; however, in the other samples the g-ratio plateau is ~0.95 suggesting that myelin thickness increases very little or at a constant rate, in relation to increases in axon diameter >2  $\mu\text{m}$ .

The rabbit retina differs from a number of mammalian species, including humans, because of the myelination of intraretinal axons.<sup>[20,31]</sup> Similar to that seen at the ROJ in other animals, myelination within the streak is not abrupt but is feathered at its leading edge and there is a mixture of myelinated and unmyelinated axons. Myelinated retinal axon diameters were significantly larger (~30%;  $P < 0.001$ ) and had a broader range compared to unmyelinated retinal axons ( $0.27\text{-}3.02 \mu\text{m}$  vs.  $0.15\text{-}1.36 \mu\text{m}$ , respectively; see Fig. 6) and were comparable to human IRM patches and the ROJ. Myelin thickness ( $0.11 \pm 0.04$ ,  $n = 412$ ) was positively correlated with axon size ( $y = 0.042 + 0.07x$ ,  $r^2 = 0.272$ ;  $P < 0.0001$ ) and the mean g-ratio ( $0.80 \pm 0.06$ ,  $n = 412$ ) was not significantly different compared with the two human specimens (the curves also peak and plateau at about the same level).

## Discussion

We show that IRM axonal diameters are on average larger than non-myelinated axons from the same population and suggest that glial cells (possibly oligodendrocytes) can induce diameter changes in retinal axons that would normally remain unmyelinated. A comparison of IRM with that normally occurring at the ROJ and ON suggests that the effect is more dramatic on the intraretinal portion of the axon compared with the ON and that these changes are abnormal.

Axon diameter, whether sampled along the unmyelinated intraretinal portion or along the myelinated ON, does not remain constant and there is a gradual increase in diameter

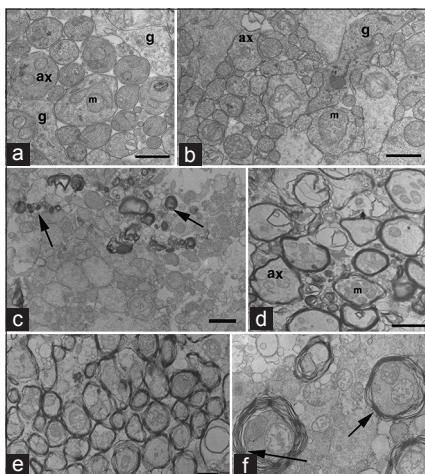


**Figure 2:** (a) Ganglion cell axons from normal temporal retina (S843; 77-year-old female, 20-h fixation delay) can be compared to unmyelinated axons of S694 (b; R1, Fig. 3). Note, axons (ax) in A and B show no signs of degeneration; preservation was sufficient to see neurofilaments, mitochondria (m) and glia (g). (c) Micrograph shows scattered myelinated axons (arrows; S694 R1). (d) Myelinated axons (S694; R2, Fig. 3). (e and f) myelinated axons of the central region of S656 (R2 Fig. 4). Arrows show areas measured for axons with separated lamella. Scale bar; A, B- 0.5 $\mu\text{m}$ ; C, E- 1.0  $\mu\text{m}$ ; D, F- 2.0  $\mu\text{m}$

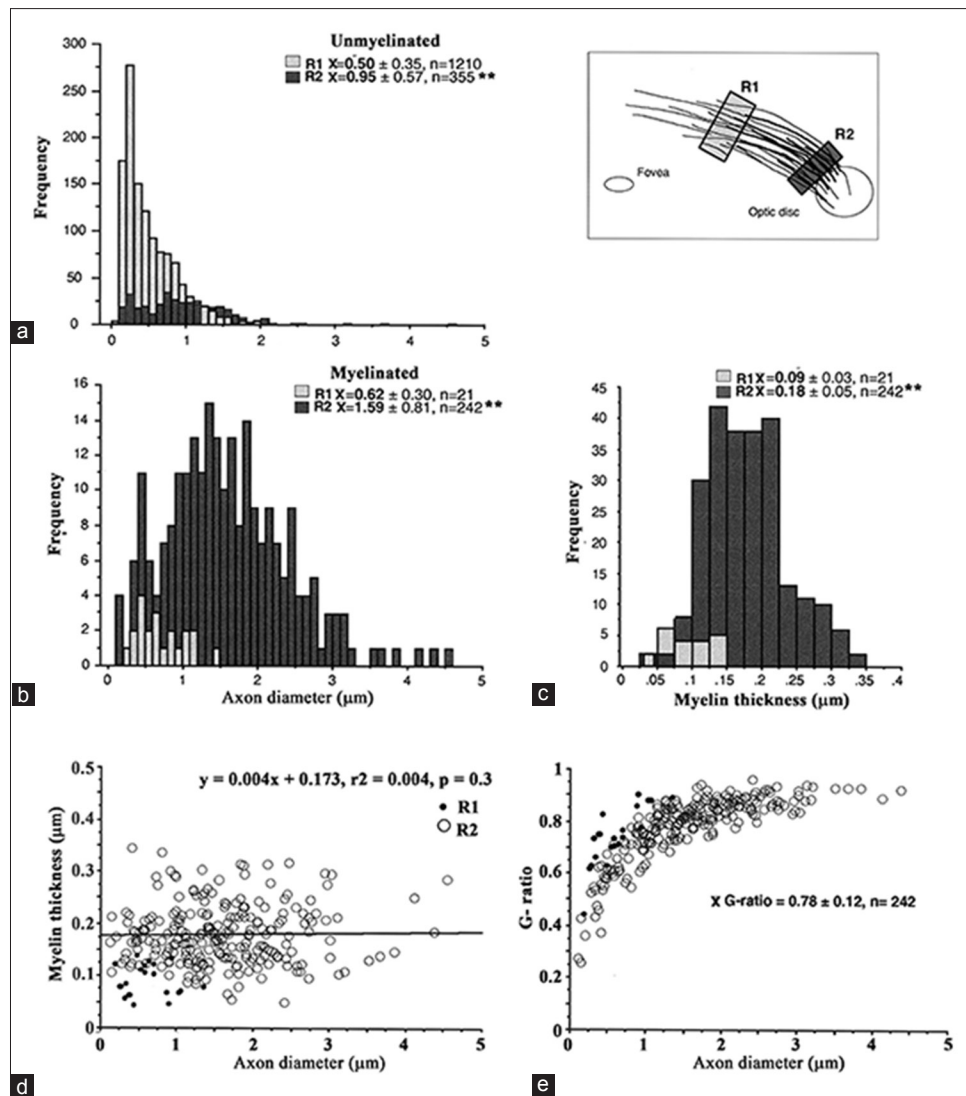


**Figure 3:** Axon diameter and myelin thickness in specimen S694. (a) Unmyelinated axon diameters were compared between two locations, one at the peripheral edge of the myelin patch (R1) and one adjacent to the optic disc (R2). (b) Myelinated axon diameters were compared between the same two locations. Axon diameters in A and B show a shift toward larger diameters in the central location (\*\* $P < 0.01$ ). (c) Myelin thickness for the two areas. (d,e) Axon diameters were not correlated to changes in myelin thickness and g-ratios reached a plateau at  $\sim 0.9$ - $0.95$ . Black dots indicate measurements for R1

between the retinal ganglion cell soma and its target nucleus.<sup>[20,32]</sup> In addition, studies in another primate, the marmoset, suggest that the rate of intraretinal axon diameter change may be related to initial size and cell class. Large parasol axons tend to increase more rapidly and to a greater extent than small parasol axons.<sup>[33]</sup> Others have reported the increase in axon diameter with myelination in the rabbit.<sup>[2,16,20]</sup> Some of the variation has also been attributed to the presence of membranous cell organelles moving along the axon.<sup>[32]</sup> Indeed, Greenberg and colleagues<sup>[32]</sup> argue that unmyelinated axons can be considered as dynamic varicose structures. However, it is clear that this cannot explain the axon size differences between the retina and ON in normal animals nor the changes seen in the present study.

Our comparison of IRM suggests that these sites more closely resemble the situation at the ROJ rather than the ON. There is no uniform front of myelination within the patches,

the ROJ or medullary streak of the rabbit. The ROJ normally represents an area of transition between unmyelinated retinal axons and myelinated ON fibers<sup>[2-5,30]</sup> and exhibits unique axo-glial relationships that are not evident in the ON. Myelinated axons in this region have unusually thin myelin sheaths and do not show several of the correlations reported for the ON (e.g., internodal distance, number of myelin lamellae).<sup>[2,14,26]</sup> Similarly, during rat ON development, ensheathed axons (oligodendroglial envelopment prior to myelin compaction) show an axonal diameter that is intermediate between myelinated and naked axons.<sup>[34]</sup>

Several authors have highlighted the correlations between axon diameter and a number of parameter (e.g., myelin thickness).<sup>[12-14,20,30]</sup> In general, larger axons have thicker myelin sheaths and correspondingly more lamellae, although this is not always the case; small axons may have relatively thick myelin, and the converse (large axons/thin myelin) as observed in the

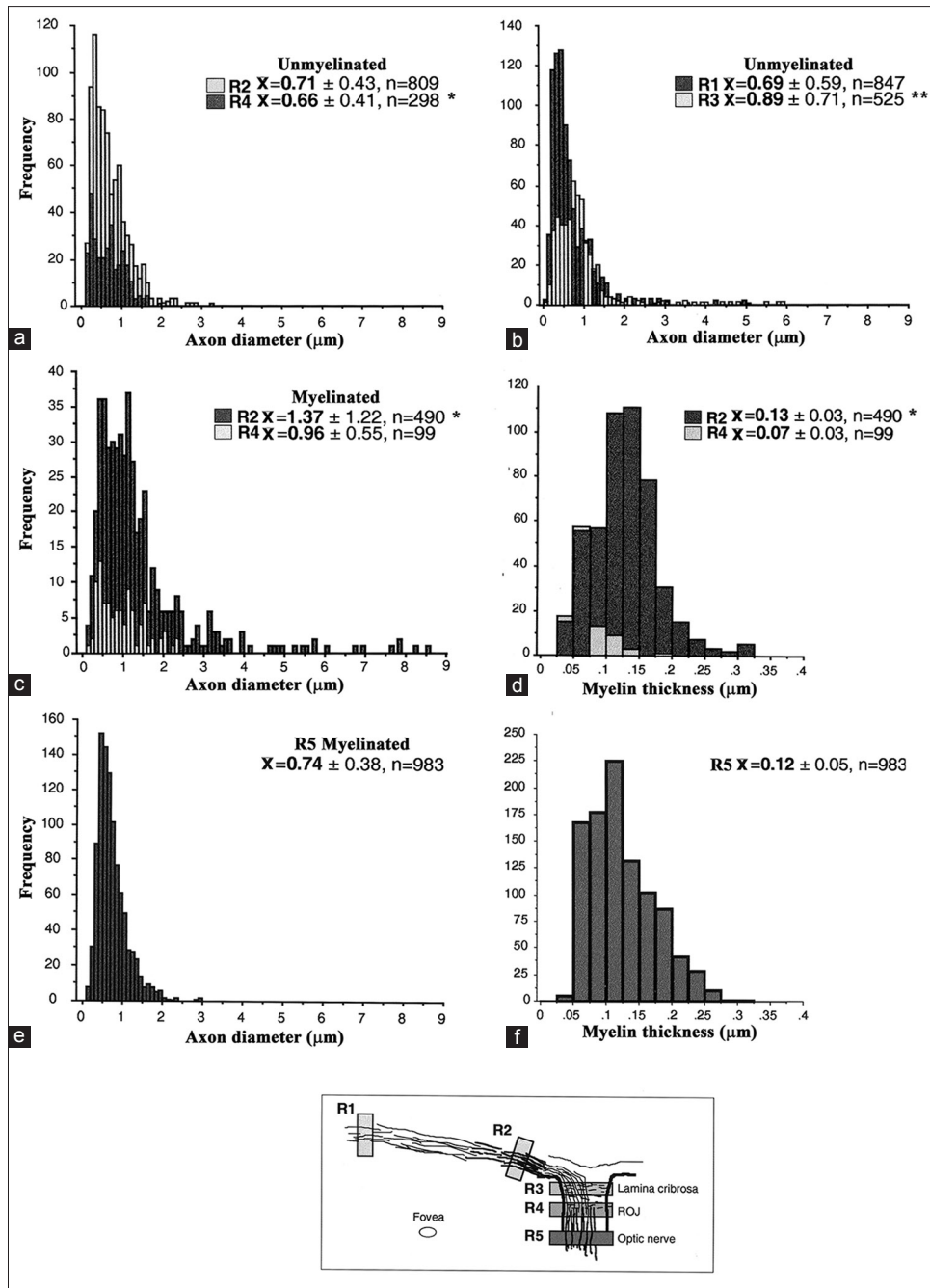


**Figure 4:** Analysis of axon diameter and myelin thickness in specimen S656. (a, b) The distribution of unmyelinated axon diameters at the three locations shown in the schematic diagram (R1 vs. R2 was not significant). (c, d) The distribution of myelinated axon diameters at three locations are shown (R5 vs. R2\*\*, R5 vs. R4\*\*). (e, f) The distribution of myelin thickness for the same areas (R5 vs. R4\*, R5 vs. R2 ns). \* $P < 0.05$ ; \*\* $P < 0.01$ , ns- nonsignificant (t-test). ROJ corresponds to the retinal optic-nerve junction

present study and by others.<sup>[20,30]</sup> Our data suggests that in the human this relationship is not particularly strong as the g-ratios plateau at ~ 1.5-2  $\mu\text{m}$  suggesting that myelin thickness shows only a small increase with axons  $> 2 \mu\text{m}$ .<sup>[29,30]</sup> G-ratios within the IRM patches more closely resembled those seen within the rabbit, cat and guinea pig ON,<sup>[20,29,30]</sup> while the ROJ g-ratio is higher than ON ratio (present study and other species). The lower ON g-ratio of S843 can in part be explained by the number of smaller foveal fibers, which appear to have proportionately thicker myelin sheaths compared to more peripheral populations.<sup>[27]</sup>

It is unclear whether these cases represent a stage of stable myelination or unstable recurrent de- and re-myelination.<sup>[23]</sup> Hunter *et al.*,<sup>[7]</sup> suggested that myelination advances from the edges of the patch over time and that new oligodendrocytes are produced from an early clonal progeny containing two different behaviors (migratory and nonmyelinating followed by mature nonmigratory behavior and myelin formation). The lack of continuous myelination between the retina and ON suggests either a stable oligodendrocyte population or may reflect the normal inhibitory nature of the lamina cribrosa to

oligodendrocyte migration in the ROJ and ON or interactions with astrocytes.<sup>[4]</sup> Axons of the CNS that undergo remyelination in the mouse typically have decreased internodal distances and a decrease in myelin thickness and g-ratios.<sup>[26]</sup> Myelin mutants such as the 'rumpshaker' mouse show a similar picture of hypomyelination of large fibers but essentially normal myelination of small fibers.<sup>[35]</sup> In contrast, early remyelination after a pressure block of the cat's ON caused a hypermyelination (thicker myelin) than that seen after long recovery periods.<sup>[29]</sup>

Our data suggests that both unmyelinated and myelinated axons are larger than normal within the more densely myelinated regions and this may be due to a diffusible factor (s). Conversely, this may reflect the fact that oligodendrocyte

induced axonal diameter changes affect unmyelinated portions of the same axon for some distance on either side of the IRM. The more densely myelinated patches may exhibit greater differences in size compared to smaller or less dense patches due to the higher concentrations of diffusible factors in the local area and a higher number of direct contacts with glial cells within the patch. Thus, this appears to be a graded response to the presence of the glial cells. It has been suggested that the larger premyelinated axons and the frayed or striated border of myelination within the rabbit is consistent with a diffusible substance<sup>[3,12,20]</sup> and that oligodendrocyte interactions, either through soluble factors or direct contact, may affect an increase in the amount of neurofilament phosphorylation.<sup>[12,36,37]</sup> In the mouse ON, there is a sudden rise in axon calibre and

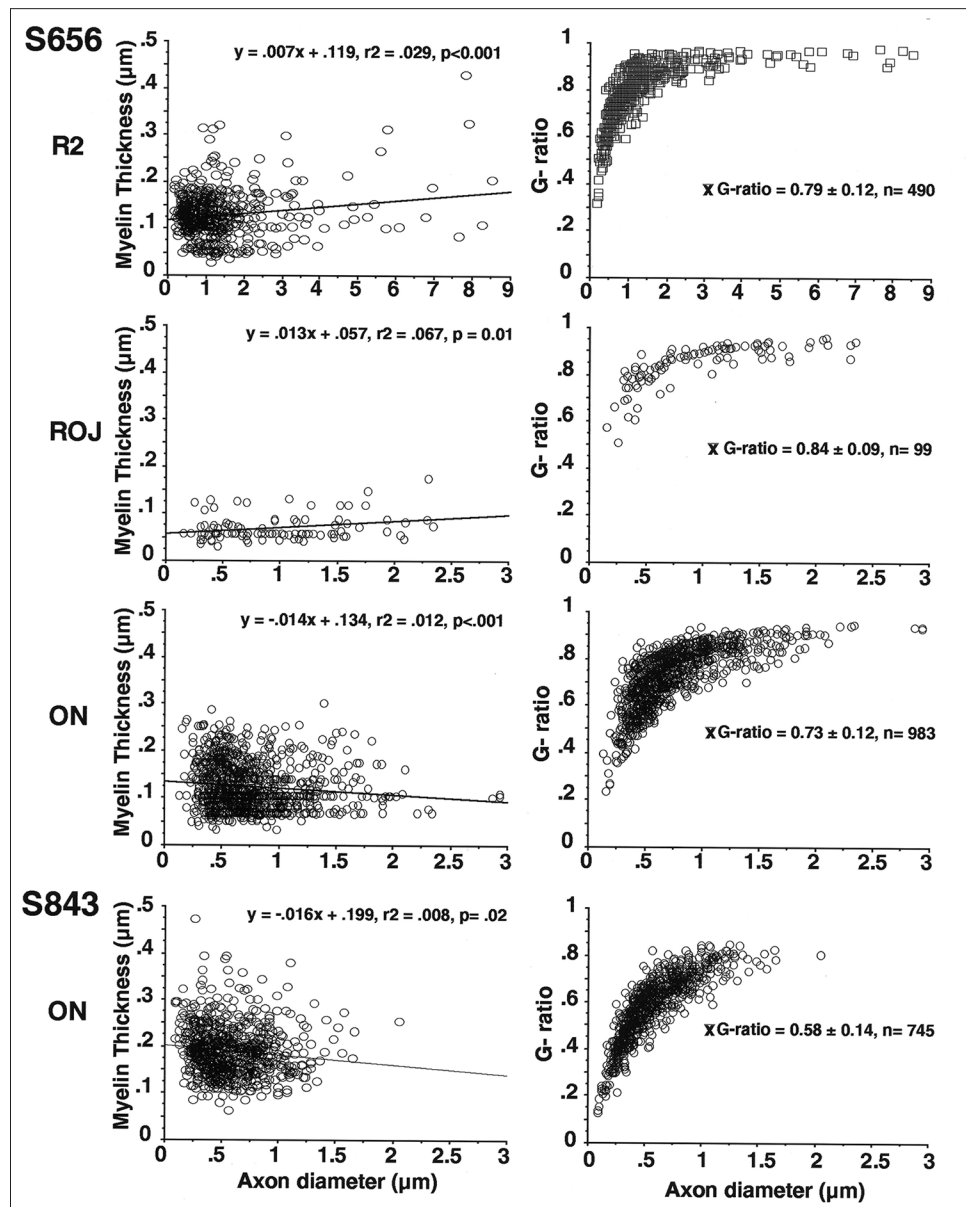


**Figure 5:** Myelin thickness versus axon diameter and associated g-ratios. Myelin thickness showed significant correlations to axon diameter for each of the sample locations shown in Figure 4 (S656). In contrast to the retinal sample locations, myelin thickness showed a significant negative correlation in the two optic nerves sampled (S843 represents a normal optic nerve, see also Figure 2). The associated g-ratios are shown for the same sample locations. Note that in the majority of cases g-ratios plateaued at ~0.9



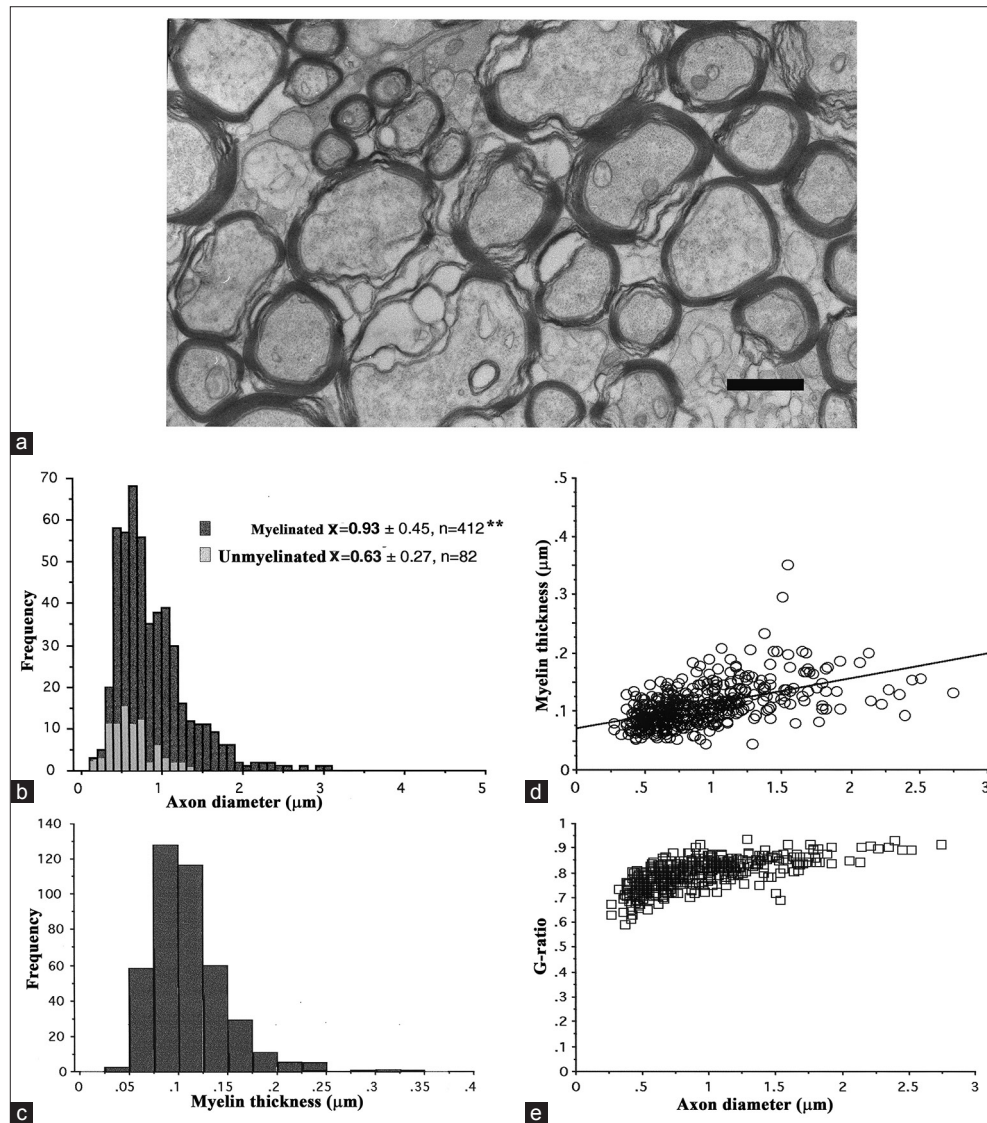


**Figure 6:** Comparison data taken from the rabbit retina. (a) Myelinated axons (ax) in the medullary ray (scale bar = 1  $\mu\text{m}$ ). (b) Size comparison of unmyelinated and myelinated axons. Note the broader range of axon diameters for myelinated axons. (c) Myelin thickness for the same axons (mean  $0.11 \pm 0.04 \mu\text{m}$ ,  $n = 412$ ). (d, e) Axon diameter showed a significant positive correlation with myelin thickness ( $y = 0.042 + 0.07x$ ,  $r^2 = 0.272$ ,  $P = 0.0001$ ) and mean g-ratio of  $0.80 (\pm 0.06)$ ,  $n = 412$ ). Note the narrow range of rabbit g-ratios compared with human data, although the plateau values were very similar

neurofilament number just as the axon becomes myelinated<sup>[12,38]</sup> and although unmyelinated axon calibre remains unchanged, interneurofilament spacing increases with distance from the eye suggesting some indirect effect of myelination in neighboring axons. Although oligodendrocytes can still trigger caliber expansion without ON myelin,<sup>[12]</sup> Brady *et al.*,<sup>[18]</sup> suggested that formation of compact myelin is necessary for the normal differentiation of large axons but simple oligodendrocyte/axon contact is not sufficient.<sup>[14,15,17-19,36]</sup>

Oligodendrocyte progenitor cells transplanted into the normal rat retina cause a massive myelination of ganglion cell axons and these axons have a normal morphology.<sup>[39]</sup> Freshly isolated syngeneic 3-week-old rat cerebellar oligodendrocytes also survive, mature, and express a myelin-specific protein when transplanted into 4-day old rat retina in a pattern

consistent with myelination of ganglion cell axons.<sup>[40]</sup> In contrast, the IRM in our specimens does not appear to be normal. However, adult oligodendrocytes are phenotypically heterogeneous, and phenotypic type appears to be related to axon diameter and activity within the axon.<sup>[14]</sup> The range of axon diameter in the patches also appears to be abnormally broad and this combined with changes in axonal activity such as salutatory action potential conduction, action potential block, or retinal ganglion cell activity, may produce an interaction between the glial cells and the axon that results in an abnormal phenotype and myelination. Previous studies have noted a number of functional visual problems in patients with intraretinal myelination<sup>[8]</sup> but it is not clear if this is due the myelin or other factors. Given the position of the IRM patches large areas of the retina peripheral to the IRM could potentially be affected.<sup>[22]</sup>

Myelination is known to speed up conduction velocity in axons;<sup>[25]</sup> however, whether IRM alters conduction velocity or blocks axonal conduction remains to be clarified and these issues may have different clinical outcomes. Stanford<sup>[41]</sup> suggested that conduction velocity alterations along the visual pathway produced an almost constant transmission time from retinal ganglion cell to central targets and this was important for minimizing spatiotemporal dispersion and maintaining the spatiotemporal representation of the image. Previous work has shown that retinal ganglion cell axon sizes does not remain constant<sup>[33,42]</sup> and the variation in some parasol cells could lead to conduction velocity changes of ~0.2-0.3 m/s in first 2 mm of intraretinal length.<sup>[33]</sup> These differences may be necessary to minimize spatiotemporal dispersion for accurate perception (in particular motion). The well known Pulfrich Effect<sup>[43]</sup> has been used to demonstrate the binocular effects of altering the temporal dynamics between the two eyes, and temporal factors are also thought to be important in high acuity demonstrated by vernier offset experiments.<sup>[44,45]</sup> Thus, patients with IRM may present with subtle perceptual problems that are related to the altered conduction velocities, which may be particularly noticeable for binocular interactions. The lack of complete IRM across the thickness of the fiber layer suggests that the effects of IRM would encompass large retinal sectors due to the lack of specific axonal organization within the nerve fibre layer.<sup>[22]</sup> If the IRM is an ongoing case of myelination and myelin removal, the patient may present with variable visual difficulties on the course of clinical examination and lead to some frustration by the clinician as to the their cause. The rarity of human samples available for detailed study make conclusions difficult but clearly further research may yield additional insights into the complex interactions between oligodendrocytes and their targets and how this may affect the function of visual system.

## Acknowledgments

This work was supported by grants from the Sydney Hospital Foundation for Research.

## References

- Berliner ML. Cytologic studies on the retina. Normal coexistence of oligodendroglia and myelinated nerve fibres. *Arch Ophthalmol* 1931;6:740-51.
- Hildebrand C, Remahl S, Waxman SG. Axo-glia relations in the retina-optic nerve junction of the adult rat: Electron- microscopic observations. *J Neurocytol* 1985;14:597-617.
- Perry VH, Lund RD. Evidence that the lamina cribrosa prevents intraretinal myelination of retinal ganglion cell axons. *J Neurocytol* 1990;19:265-72.
- Ffrench-Constant C, Miller RH, Burne JF, Raff MC. Evidence that migratory oligodendrocyte-type 2 astrocyte (O-2A) progenitor cells are kept out of the rat retina by a barrier at the eye-end of the optic nerve. *J Neurocytol* 1988;17:13-25.
- Duke-Elder S. Normal and abnormal development. Medullated nerve fibers. In: Duke-Elder S, editor. *System of Ophthalmology*. Vol. 3. London: Henry Kimpton; 1964. p. 646-51.
- Leys AM, Leys MJ, Hooymans JM, Craandijk A, Malenfant M, Van Germeersch D, et al. Myelinated nerve fibers and retinal vascular abnormalities. *Retina* 1996;16:89-96.
- Hunter SH, Leavitt JA, Rodriguez M. Direct observation of myelination *in vivo* in the mature human central nervous system: A model for the behaviour of oligodendrocyte progenitors and their progeny. *Brain* 1997;120:2071-82.
- Perry VH, Hayes L. Lesion-induced myelin formation in the retina. *J Neurocytol* 1985;14:297-307.
- Straatsma BR, Heckenlively JR, Foos RY, Shahinian JK. Myelinated retinal nerve fibres associated with ipsilateral myopia, amblyopia, and strabismus. *Am J Ophthalmol* 1979;88:506-10.
- Straatsma BR, Foos RY, Heckenlively JR, Taylor GN. Myelinated retinal nerve fibers. *Am J Ophthalmol* 1981;91:25-38.
- Williams TD. Medullated retinal nerve fibers: Speculations on their cause and presentation. *Am J Optom Physiol Opt* 1986;63:142-51.
- Sánchez I, Hassinger L, Paskevich PA, Shine H, Nixon RA. Oligodendroglia regulate the regional expansion of axon caliber and local accumulation of neurofilaments during development independently of myelin formation. *J Neurosci* 1996;16:5095-105.
- Bray GM, Rasminsky M, Aguayo AJ. Interactions between axons and their sheath cells. *Annu Rev Neurosci* 1981;4:127-62.
- Butt AM, Berry M. Oligodendrocytes and the control of myelination *in vivo*: New insights from the rat anterior medullary velum. *J Neurosci Res* 2000;59:477-88.
- Dangata YY, Kaufman MH. Myelinogenesis in the optic nerve of (C57BL X CBA) F1 hybrid mice: A morphometric analysis. *Eur J Morphol* 1997;35:3-17.
- Vaney DI. A quantitative comparison between the ganglion cell populations and axonal outflows of the visual streak and periphery of the rabbit retina. *J Comp Neurol* 1980;189:215-33.
- Yin X, Crawford TO, Griffin JW, Tu PH, Lee VM, Li C, et al. Myelin-associated glycoprotein is a myelin signal that modulates the caliber of myelinated axons. *J Neurosci* 1998;18:1953-62.
- Brady ST, Witt AS, Kirkpatrick LL, de Waegh SM, Readhead C, Tu PH, et al. Formation of compact myelin is required for maturation of the axonal cytoskeleton. *J Neurosci* 1999;19:7278-88.
- Ishibashi T, Ikenaka K, Shimizu T, Kagawa T, Baba H. Initiation of sodium channel clustering at the node of Ranvier in the mouse optic nerve. *Neurochem Res* 2003;28:117-25.
- Reichenbach A, Schippel K, Schumann R, Hagen EJ. Ultrastructure of rabbit retinal nerve fibre layer-Neuroglial relationships, myelination, and nerve fibre spectrum. *J Hirnforsch* 1988;29:481-91.
- Provis JM, Penfold PL, Edwards AJ, van Driel D. Human retinal microglia: Expression of immune markers and relationship to the glia limitans. *Glia* 1995;14:243-56.
- FitzGibbon T, Taylor SF. Retinotopy of the human retinal nerve fibre layer and optic nerve head. *J Comp Neurol* 1996;375:238-51.
- FitzGibbon T, Nestorovski Z. Morphological consequences of myelination in the human retina. *Exp Eye Res* 1997;65:809-19.
- Halasz P, Martin PR. A microcomputer based system for semi-automatic analysis of histological sections. *Proc R Microsc Soc* 1984;19:312.
- Sadun AA, Bassi CJ. Optic nerve damage in Alzheimer's Disease. *Ophthalmology* 1990;97:9-17.
- Miller DJ, Rodriguez M. Spontaneous and induced remyelination in multiple sclerosis and the Theiler's virus model of central nervous system demyelination. *Microsc Res Tech* 1995;32:230-45.
- FitzGibbon T, Taylor SF. Mean retinal ganglion cell axon diameter varies with location in the human retina. *Jpn J Ophthalmol* 2012;56:631-7.
- Sadun AA, Johnson B, Miao M. Axon caliber populations in the human optic nerve: Changes with age and disease. *Proceedings of the Sixth Meeting of the International Neuro-Ophthalmology Society*; 1987. p. 15-20.
- Cottee LJ, Daniel C, Loh WS, Harrison BM, Burke W. Remyelination and recovery of conduction in cat optic nerve after demyelination by pressure. *Exp Neurol* 2003;184:865-77.
- Guy J, Ellis A, Kelley K, Hope MG. Spectra of g ratio, myelin sheath



- thickness, and axon and fiber diameter in the guinea pig optic nerve. *J Comp Neurol* 1989;287:446-54.
31. Vaney DI, Hughes A. The rabbit optic nerve: fibre diameter spectrum, fibre count, and comparison with a retinal ganglion cell count. *J Comp Neurol* 1976;170:241-52.
  32. Greenberg MM, Leitao C, Trgadis J, Stevens JK. Irregular geometries in normal unmyelinated axons: A 3D serial EM analysis. *J Neurocytol* 1990;20:978-88.
  33. Walsh N, Ghosh KK, FitzGibbon T. Intraretinal axon diameters of a New World primate, the marmoset (*Callithrix jacchus*). *Clin Exp Ophthalmol* 2000;28:423-30.
  34. Black JA, Waxman SG, Ransom BR, Feliciano MD. A quantitative study of developing axons and glia following altered gliogenesis in rat optic nerve. *Brain Res* 1986;380:122-35.
  35. Lunn KF, Fanarraga ML, Duncan ID. Myelin mutants: New models and new observations. *Microsc Res Tech* 1995;32:183-203.
  36. Bauer NG, Richter-Landsberg C, Ffrench-Constant C. Role of oligodendroglial cytoskeleton in differentiation and myelination. *Glia* 2009;57:1691-705.
  37. Nakagawa T, Chen J, Zhang Z, Kanai Y, Hirokawa N. Two distinct functions of the carboxyl-terminal tail domain of N F-M upon neurofilament assembly: Cross-bridge formation and longitudinal elongation of filaments. *J Cell Biol* 1995;129:411-29.
  38. Nixon RA, Paskevich PA, Sihag RK, Thayer CY. Phosphorylation on carboxyl terminus domains of neurofilament proteins in retinal ganglion cell neurons *in vivo*: Influences on regional neurofilament accumulation, interneurofilament spacing, and axon caliber. *J Cell Biol* 1994;126:1031-46.
  39. Leang P, Molthagen M, Yu EG, Bartsch U. Transplantation of oligodendrocyte progenitor cells into the rat retina: Extensive myelination of retinal ganglion cell axons. *Glia* 1996;18:200-10.
  40. Huang PP, Alliquant B, Carmel PW, Freidman ED. Myelination of the rat retina by transplantation of oligodendrocytes into 4-day-old hosts. *Exp Neurol* 1991;113:291-300.
  41. Stanford LR. Conduction velocity variations minimize conduction time differences among retinal ganglion cell axons. *Science* 1987;238:358-60.
  42. Walsh N, FitzGibbon T, Ghosh KK. Intraretinal axon diameter: A single cell analysis in the marmoset (*Callithrix jacchus*). *J Neurocytol* 1999;28:989-98.
  43. Morgan MJ, Thompson P. Apparent motion and the Pulfrich effect. *Perception* 1975;4:3-18.
  44. Berkley MA, Sprague JM. Striate cortex and visual acuity functions in the cat. *J Comp Neurol* 1979;187:679-702.
  45. Swindale NV, Cynader MS. Vernier acuity of neurones in cat visual cortex. *Nature* 1986;319:591-3.
- Cite this article as:** FitzGibbon T, Nestorovski Z. Human intraretinal myelination: Axon diameters and axon/myelin thickness ratios. *Indian J Ophthalmol* 2013;61:567-75.
- Source of Support:** This work was supported by grants from the Sydney Hospital Foundation for Research. **Conflict of Interest:** None declared.